The relationship between ethylene-induced autophagy and reactive oxygen species in *Arabidopsis* root cells during the early stages of waterlogging stress

Qiwei Zheng[1], Gege Li[1], Hongyan Wang[1], Zhuqing Zhou[1]

[1] Laboratory of Cell Biology, College of Life Science and Technology, Huazhong Agricultural University, Wuhan, China

Corresponding Author: Zhuqing Zhou

Correspondence address: Laboratory of Cell Biology, College of Life Science and Technology, Huazhong Agricultural University, Wuhan, China

Email address: zhouzhuqing@mail.hzau.edu.cn

Abstract

The response of plants to waterlogging stress is a complex process, with ethylene playing a crucial role as a signaling molecule. However, it remains unclear how ethylene is initially triggered in response to waterlogging stress when plants are continuously waterlogged for less than 12 hours. Here, we have shown that ethylene-induced autophagy leads to the degradation of damaged mitochondria (the main organelles producing reactive oxygen species (ROS)) to reduce ROS production during oxidative stress in *Arabidopsis thaliana*, which improves the survival rate of root cells in the early stages of waterlogging stress. Waterlogging stress activated ethylene-related genes, including *ACO2*, *ACS2*, *ERF72*, *ERF73*, and *EIN3*, and ethylene content of plants increased significantly within 24 h of continuous waterlogging. As stress duration increased, increased amounts of ROS accumulated in *Arabidopsis thaliana* roots, and the activity of antioxidant enzymes initially increased and then decreased. Concurrently, the level of ethylene-induced autophagy, which participates in antioxidant defense, is higher in wild-type plants than in the octuple *acs* mutant *cs16651* (*acs2-1/acs4-1/acs5-2/acs6-1/acs7-1/acs9-1/amiRacs8acs11*). Exogenous application of 1-aminocyclopropanecarboxylic acid (ACC), resulted in a more pronounced manifestation of autophagy in the stele of *Arabidopsis* roots. Compared with the waterlogging treatment group or the ACC treatment group, the waterlogging + ACC treatment can induce autophagy to occur earlier and expand the autophagic range to the epidermis of *Arabidopsis thaliana* roots. Overall, our results provide insight into the important role of ethylene-induced autophagy in enhancing the antioxidative capacity of *Arabidopsis thaliana* during the early stages of waterlogging stress. Furthermore, we suggest ethylene as a potential candidate for mitigating the deleterious effects caused by waterlogging in *Arabidopsis thaliana*.

Introduction

During the growth process, plants face various abiotic stressors such as drought, salt, and flooding stress. These stressors can cause energy and carbohydrate crises in plants, limit plant growth and development, and lead to a decline in crop yield and quality (Zhu, 2016). Soil

38 flooding creates a hypoxic environment (Phukan, Mishra & Shukla, 2016). Plants undergo two

39 important changes during waterlogging: an increase in ROS and the gaseous plant hormone

40 ethylene. Waterlogging-tolerant plants use changes in O_2, ROS, and ethylene as signals to induce

41 adaptive processes (Voesenek & Sasidharan, 2013).

42 The ethylene content in *Arabidopsis* root tips increases rapidly after submergence (Perata, 2020).

43 Ethylene insensitive protein 3 (EIN3) is an important transcription factor that mediates the

44 ethylene response (Xie et al., 2015; Hartman et al., 2019). Multiple studies have shown that

45 ethylene is critical in hypoxia and metabolic adaptation during plant flooding and can adapt to

46 hypoxia by enhancing the stability of ethylene-responsive factor family VII (ERF-VIIs) (Chen et

47 al., 2015a; Yao et al., 2017; Hartman, Sasidharan & Voesenek, 2021). ERFs are involved in

48 hormones, development, metabolic adaptation, and abiotic stress responses. Ethylene response

49 factor 74 (ERF74) can activate the expression of respiratory burst oxidase homolog D

50 (RbohD)by binding to the promoter of RbohD to induce ROS production (Yao et al., 2017).

51 ROS homeostasis in plants modulates metabolic responses, contributes to morphological fitness,

52 and increases the likelihood of plant survival under flooding stress (Yeung, Bailey-serres &

53 Sasidharan, 2019). In maize, ethylene can upregulate the expression of ZmEREB180, which is

54 closely related to waterlogging tolerance (Yu et al., 2019).

55 ROS, as metabolic byproducts and secondary messengers, play an important role in growth,

56 development, and programmed cell death in response to the environment (Suzuki et al., 2011;

57 Liu & He, 2016). In higher plants, ROS are produced in various subcellular structures during

58 plant growth and development, including mitochondrial respiration, chloroplast photosynthesis,

59 peroxisomes, and NADPH oxidase (respiratory burst oxidase homologues) located on the plasma

60 membrane (Waszczak, Carmody & Kangasjärvi, 2018). During waterlogging, the formation of

61 ROS is a common physiological process in plants (Mu et al., 2007; Iskandar & Mahmood, 2010;

62 Parlanti et al., 2011). When plants are exposed to various environmental stressors, the content of

63 ROS in plants increases, causing damage to lipids, proteins, and DNA (Gill & Tuteja, 2010;

64 Wang et al., 2018a). Plants have evolved corresponding antioxidant systems to remove excess

65 ROS and protect them from oxidative damage. For example, superoxide dismutase (SOD)

66 converts superoxide anion radicals ($O_2^{\cdot-}$) into H_2O_2 and catalase (CAT) converts H_2O_2 into H_2O

67 and O_2. Ascorbate peroxidase (APX) relieves the toxic side effects of H_2O_2, and glutathione

68 reductase (GR)participates in metabolic regulation and antioxidant processes (Morel &

69 Barouki, 1999; Foyer & Noctor, 2003; Iskandar & Mahmood, 2010).

70 Autophagy is a conserved process that decomposes misfolded proteins or toxic substances and
71 damaged organelles into biological macromolecules (such as amino acids and fatty acids) for
72 recycling to maintain eukaryotic growth, development, and survival (Li & Vierstra, 2012; Wang,
73 Mugume & Bassham, 2018). Normally, autophagy occurs at very low levels, but the process is
74 activated under various environmental cues (Marshall & Vierstra, 2018). Studies have shown
75 that to resist waterlogging stress, autophagy can balance energy and ensure basic metabolism in
76 plants (Chen et al., 2015b). Mitophagy is an adaptive regulation that is critical for reducing ROS
77 levels and preventing cell death when mammalian cells are chronically hypoxic (Zhang et al.,
78 2008). Although mitophagy is less frequently reported in plants, it can recycle damaged
79 mitochondria during abiotic stress (Ma et al., 2021; Nguyen & Lazarou, 2021). Studies have
80 shown that autophagy plays an important role in ethylene-mediated drought tolerance.
81 Autophagy induced by ROS levels, dependent on mitochondrial alternating oxidase (AOX), is
82 critical for ethylene-mediated drought tolerance in tomato. ERF5 binds to the promoters of
83 autophagy-related genes (ATGs) ATG8d and ATG18h and is critical for ethylene-induced
84 autophagosome formation in tomato under drought conditions (Zhu et al., 2018). Another study
85 showed that ethylene mediates the induction of GmATG8i in soybean plants under starvation
86 stress (Okuda et al., 2011). Ethylene signaling is involved in autophagy in response to stress by
87 inducing ATGs gene expression and altering ROS levels, but only in energy crises caused by
88 insufficient carbohydrate reserves (Hartman, Sasidharan & Voesenek, 2021). Ethylene and ROS
89 can enhance hypoxia resistance in wheat seedlings by controlling morphological adaptation and
90 metabolic responses (Yamauchi et al., 2014). Under hypoxic conditions, root cortex cells induce
91 RbohD translation to increase ROS production, which plays an important role in ethylene-
92 induced stomatal formation in rice roots (Yamauchi et al., 2017). Some studies suggest that
93 ethylene plays an important role in the induction of autophagy, thereby improving the survival
94 rate under flooding and hypoxia stress (Hartman, Sasidharan & Voesenek, 2021).
95 While we speculate that ethylene may be involved in hypoxia-mediated autophagy
96 under waterlogging stress, we also propose that in plants, mitophagy can be activated by
97 ethylene-dependent ROS production, which may have a negative regulatory effect on ROS
98 production.
99 **Materials & Methods**
100 **Experimental materials and growth conditions**

101 The wild-type (WT)*Arabidopsis* used in this study was Columbia-0 (Col-0). *Rbohd/f*, octet

102 *acs* mutant (*CS16651*, *acs2-1/acs4-1/acs5-2/acs6-1/acs7-1/acs9-1/amiRacs8acs11*), *ein2-5*,

103 *p35S::EIN3-GFP*, and *ein3/eil1-1* (Lv et al., 2018) were presented by Professor Ding Zhaojun of

104 Shandong University. *ATG8epro::GUS* (Guan et al., 2019) was obtained from our laboratory.

105 Before germination, the seed surface was sterilized with 5% sodium hypochlorite NaClO +

106 0.05% TWEEN-20 solution for 12 minutes, washed with sterile water 5 times, and vernalized at

107 4 °C for 3 days. Then, the seeds were sown on 1/2 MS medium and cultured in a growth room

108 (16/8 h light/dark at 22 °C /19 °C and 70% relative humidity) for 7 days.

109 **Experimental design**

110 Waterlogging Treatment (WL): According to the method (Wang et al., 2020), the waterlogging

111 treatment was carried out with slight modification. Seven-day-old seedlings were transferred

112 from 1/2 MS medium to a Petri dish filled with distilled water and placed in a growth chamber

113 under controlled conditions so that the roots of *Arabidopsis* seedlings are completely immersed

114 in distilled water. The leaves were kept 0.5 cm above the water surface.

115 ACC Treatment (ACC): Seven-day-old seedlings were transferred to 1/2 MS medium

116 supplemented with 0.05 μM ACC (Sigma).

117 WL+ACC Treatment (WL+ACC):After diluting the ACC stock solution to a concentration

118 of 0.05 μM with distilled water, 7-day-old seedlings were transferred from 1/2 MS medium to

119 1/2 MS medium containing 0.05 μM ACC. The seedlings were placed in a growth chamber with

120 their roots completely submerged in the 0.05 μM ACC solution, while their leaves were kept 0.5

121 cm above the water surface. All treatments were performed in three independent biological

122 replicates.

123 **Ethylene measurements**

124 The method (Sun et al., 2017) was slightly modified to determine the ethylene content, as

125 described above. Seven-day-old seedlings were randomly selected, with 30 of them transferred to

126 a 25 mL vial containing 3 mL of liquid MS medium. The vial was then sealed with a rubber

127 stopper and left for 12 h at 22°C before measuring the ethylene content. A gas-tight syringe was

128 used to draw 1 mL of the upper air sample from each bottle through the septum, which was

129 immediately injected into a GDX-502 column (2 m * 1/8 inch) and flame ionization detector

130 (FID) gas chromatograph (Agilent 7890BGC, Agilent Technologies, USA). Nitrogen (N_2) was

131 used as the carrier gas and separation was performed at 90 °C. The ethylene peak area was

132   integrated with Agilent ChemStation, and the result was expressed as the average relative

133   ethylene production (%) of each treatment.

134   **ROS assays**

135   Nitro Blue Tetrazolium Chloride monohydrate (NBT) and 3,3'-diaminobenzidine (DAB) staining

136   were performed according to the method (Kumar et al., 2014) with minor modifications. Seven-

137   day-old seedlings were immersed in 2 mg/mL NBT solution (Sigma) for 15 min and then washed

138   3 times with distilled water. The seedlings were photographed with a differential interference

139   microscopy (Nikon 80i Eclipse) and the staining intensity was analyzed using Image J software

140   to detect $O_2^{\cdot-}$ content. To detect H_2O_2 content, the seedlings were immersed in a 1 mg/mL DAB

141   solution (Sigma) for 2 h, washed 3 times with distilled water, and then photographed with a

142   differential interference microscopy (Nikon 80i Eclipse) and the staining intensity was analyzed

143   using Image J software to detect H_2O_2 content. ROS level was detected by H_2DCF-DA staining.

144   Seven-day-old seedlings were immersed in 10 μM H_2DCF-DA solution for 30 minutes and then

145   washed 3 times with distilled water. The seedlings were photographed with a laser scanning

146   confocal microscopy (TCS SP8, Leica) using 488 nm excitation light and 525 nm emission light,

147   and the fluorescence intensity was analyzed using Image J software.

148   **Observing autophagosomes in roots**

149   To detect autophagy levels, seven-day-old seedlings were immersed in a 0.05 mM

150   Monodansylcadaverine (MDC) solution (Sigma-Aldrich, 30432), gently shaken, and protected

151   from light for 10 minutes. The seedlings were then washed twice with phosphate-buffered saline

152   (PBS) for 5 min each. Finally, the seedlings were photographed using a laser scanning confocal

153   microscope (TCS SP8, Leica) with an excitation wavelength of 345 nm and an emission

154   wavelength of 455 nm.

155   For the GUS staining assay, seven-day-old ATG8epro::GUS seedlings were soaked in 10 mL of

156   GUS staining solution (0.1 M PBS (pH 7.0), 5 mM potassium ferricyanide, 5 mM potassium

157   ferrocyanide, 0.1% Triton X-100, 0.5 mg/mL X-Gluc) for 10 min in a vacuum system. The

158   samples were then incubated in 75% ethanol for 1 h at 37°C in the dark. Finally, the seedlings

159   were photographed using differential interference microscopy (Nikon 80i Eclipse).

160   **Antioxidant enzyme activity measurement**

161   CAT enzyme activity was calculated by measuring the absorbance at 405 nm, and SOD enzyme

162   activity was calculated by measuring the absorbance at 550 nm. The roots of seven-day-old

163   seedlings were collected and weighed, and the enzymatic activity of CAT and SOD was

164 examined using a kit (Jiancheng Institute of Bioengineering, Nanjing) according to the

165 manufacturer's instructions.

166 **RNA extraction and qRT-PCR**

167 TRIzol reagent (Invitrogen, 15596026) was used to extract total RNA from the fresh roots of

168 seven-day-old *Arabidopsis* seedlings. The cDNA template was synthesized using the PrimeScript

169 RT kit (Takara, RR047A), and qRT-PCR was performed using the Hieff® qPCR SYBR Green

170 Master Mix (Shanghai Yisheng Biotechnology Co., Ltd., China) according to the manufacturer's

171 instructions. The qRT-PCR primer sequences are provided in Appendix S1. The AtACTIN2 gene

172 was used as an internal control, and relative gene expression was calculated using the $2^{-\Delta\Delta CT}$

173 method.

174 **Transmission Electron Microscopy**

175 Prepare TEM samples with minor modifications according to the method (Guan et al., 2019).

176 *Arabidopsis* root meristems were selected and immediately cut into 3 mm long small segments,

177 then fixed with 2.5% glutaraldehyde in 0.1 M PBS (pH 7.0) at 4 °C for 12 h. The samples were

178 then rinsed 3 times with 0.1 M PBS for 10 min each time. After being fixed with 1% osmium

179 tetroxide for 3 h, the samples were again rinsed 3 times with 0.1 M PBS for 10 min each time.

180 The samples were dehydrated in a graded acetone series of 30%, 50%, 70%, 80%, 90%, and

181 100% (three times each, for 15 min per step) and embedded in SPI-PON 812 resin. Ultrathin

182 sections (70 nm) were prepared on an ultramicrotome (Leica EM UC7, Germany) with a

183 diamond knife and collected on Formvar-coated grids. To enhance the image contrast, the

184 sections were stained with 2% uranyl acetate and lead citrate. Finally, the cell ultrastructure was

185 observed using a transmission electron microscopy (Hitachi H-7650, Japan).

186 **Cell viability test**

187 Seven-day-old seedlings were soaked in 10 mL propidium iodide (PI) solution for 10 min and

188 photographed with a laser scanning confocal microscopy (TCS SP8, Leica) using an excitation

189 wavelength of 488 nm and an emission wavelength of 660 nm. Seven-day-old seedlings were

190 soaked in 20 µM fluorescein diacetate (FDA) solution and treated at 37°C for 10 min.

191 Subsequently, the seedling were photographed with a laser scanning confocal microscopy (TCS

192 SP8, Leica) using an excitation wavelength of 480 nm and an emission wavelength of 530 nm.

193 **Statistical Analysis**

194 All the experiments were performed in triplicate or more unless otherwise indicated, and the

195 results reported in this study are presented as the mean ± SD. Data were analyzed by a two-tailed

196 Student's t-test using GraphPad Prism 7.0. The significance levels are ∗P < 0.05, ∗∗P < 0.01, and

197 ∗∗∗P < 0.001.

Results

Ethylene responds to waterlogging stress

200 To investigate the physiological regulation of ethylene in plants under waterlogging conditions,

201 an experiment was conducted to screen the ACC concentration, which revealed that 0.5 μM

202 ACC significantly inhibited the growth of *Arabidopsis* roots (Fig. 1A). Seven-day-old WT

203 seedlings were then subjected to ACC, WL, and WL+ACC treatments. The root lengths of the

204 treated groups were all significantly shorter compared to the control group (Fig. 1B), indicating

205 that both WL and ACC treatments negatively affected root growth. To analyze the changes in

206 ethylene content in plants after waterlogging, the relative ethylene content was measured at

207 different time points in the WT (Fig. 1C). The ethylene content in the WL treatment group

208 increased significantly at 24 h compared to the control group. The WL+ACC treatment group

209 had the highest ethylene content at 8 h compared to the control group. The ethylene content in

210 the ACC treatment group varied significantly at 4 h and reached its maximum at 12 h. These

211 results demonstrate that the ethylene content in *Arabidopsis* can be increased under waterlogging

212 stress. To investigate the molecular mechanism of plant ethylene response to waterlogging stress,

213 the expression levels of genes *ACO2*, *ACS2*, *ERF72*, *ERF73*, and *EIN3*, which are closely related

214 to ethylene signaling, were analyzed. The relative expression levels of these genes were

215 significantly increased in the WL and WL+ACC treatment groups, indicating that waterlogging

216 stress can enhance the expression of ethylene signaling (Fig. 1D). *ERF72* and *ERF73,* which are

217 ethylene-responsive factors associated with hypoxic stress, were significantly upregulated in the

218 WL and WL+ACC treatment groups. *ACO2* and *ACS2*, which are involved in the conversion of

219 ACC to ethylene, were significantly upregulated in the early stages of the ACC treatment group.

220 *EIN3* is an important gene downstream of the ethylene signaling pathway that is involved in

221 ethylene-induced biological responses. The *p35S::EIN3-GFP* plants were observed using laser

222 confocal microscopy under different experimental treatments. Compared to the control group,

223 the fluorescence signals of the WL and ACC treatment groups were significantly enhanced.

224 Interestingly, the fluorescence intensity of the WL+ACC group decreased at 12 h compared to

225 the WL and ACC-treated groups (Fig. S1). Therefore, both WL and ACC treatments can induce

226 EIN3 protein synthesis and regulate related physiological changes.

Ethylene induces partial ROS production and activates antioxidant enzyme system

228 Previous studies have shown that waterlogging stress can increase ROS accumulation in

229 *Arabidopsis* roots (Guan et al., 2019). To determine whether there is a regulatory relationship

230 between ethylene and ROS under waterlogging stress, we used $H_2DCFH-DA$, DAB, and NBT

231 staining methods to detect the contents of ROS, H_2O_2, and $O_2^{\cdot-}$ in WT roots after different

232 treatments (Fig. 2A). Compared to 0 h, the ROS content in the WL treatment group was

233 significantly increased at 24 h, and the ROS content in the ACC treatment group reached its

234 maximum at 12 h (Fig. 2A-d). The contents of ROS, H_2O_2, and $O_2^{\cdot-}$ in ACC and WL+ACC

235   treatment groups were significantly increased. Compared to the WL and ACC treatment groups,
236   the WL+ACC treatment group showed an earlier and more significant increase in ROS and H_2O_2
237   content (Fig. 2A-d and 2A-f). To further demonstrate the role of ethylene in inducing ROS,
238   *cs16651* mutants were submerged, and the ethylene content was measured. The ethylene content
239   produced by *cs16651* mutants under waterlogging stress for 12 hours showed no significant
240   difference compared to 0 h (*Fig. S2B*). With an increase in waterlogging time, the H_2O_2 content
241   of the *cs16651* mutants continuously increased (*Fig. S2A*). The H_2O_2 content was significantly
242   lower than that of the WT in the same treatment group (*Fig. S2a*). The H_2O_2 content in *ein3/eil1-*
243   *1* plants was continuously increased (*Fig. S2A*). The H_2O_2 content of *ein3/eil1-1* was
244   significantly lower than that of the WL treatment group at the same time point in WT (*Fig. S2a*).
245   RBOHD and RBOHF enzymes play important roles in ROS production. Under the waterlogging
246   treatment, the ethylene content of *rbohd/f* mutants was not significantly different from that of the
247   WT at the same time point (*Fig. S2B*). In the 0-24 h waterlogging period, the H_2O_2 content of the
248   *rbohd/f* mutants was lower than that of the WT in the same period but still produced a large
249   amount of H_2O_2 (*Fig. S2A*). These experiments further demonstrated that ethylene production in
250   *Arabidopsis* promotes ROS generation under waterlogging stress. When plants are subjected to
251   environmental stress, the balance of ROS is disrupted, affecting the normal metabolism and
252   regulatory functions of plants. As the ROS content of the treatment group increased, the relative
253   expression levels of the *CAT1* and *SOD1* genes were up-regulated (Fig. 2B). During the
254   treatment period from 0 to 24 h, the activities of CAT1 and SOD1 in *Arabidopsis* were higher in
255   the WL+ACC treatment group before 12 h (*Fig. S3*), indicating an earlier antioxidant role and
256   ROS scavenging. The expression of the *GST1* gene was mainly up-regulated after 12 h of
257   submersion, further exerting an antioxidant effect (Fig. 2B).

258   ## Ethylene induces partial autophagy in stele under waterlogging stress
259   Autophagy is an important physiological process for plant energy reuse. ROS induce the
260   production of autophagy when plants are waterlogged (Guan et al., 2019). *ATG8epro::GUS*
261   seedlings were stained to observe the autophagy phenomenon in *Arabidopsis* roots under
262   different treatments. In this study, autophagy appeared only in the stele in the ACC treatment
263   group, and the number of autophagosomes gradually increased as the treatment was prolonged.
264   In the WL treatment group, autophagy first occurred in the stele and then in the cortex.
265   Autophagy appeared in the WL+ACC treatment group at 4 h in the stele and cortex, and the
266   number of autophagosomes increased as the treatment time was extended (Fig. 3B). This
267   experiment showed that autophagy in the root stele of Arabidopsis was induced by ethylene
268   under waterlogging stress and that it occurred earlier than in the cortex. The MDC staining
269   experiment showed that, compared to the control group, the number of autophagosomes in the
270   three treatment groups of WT seedlings significantly increased after 24 h (Fig. 3D). Autophagy
271   gene expression was significantly up-regulated in the ACC, WL, and WL+ACC treatment
272   groups. However, during the period from 0 to 48 h, the relative expression levels of *ATG2*,
273   *ATG5*, *ATG7*, *ATG8e*, and *ATG10* in the WL+ACC group appeared earlier than those in the WL
274   group (Fig. 3A), further indicating that ethylene plays a role in inducing autophagy.

275 Ethylene-induced autophagy helps scavenge ROS produced by mitochondria

276 To further elucidate the relationship between ethylene and autophagy under waterlogging stress,

277 autophagosomes were observed using MDC staining in *ein3/eil1-1*, *cs16651*, and *rbohd/f*

278 mutants after waterlogging (Fig. 4A). At 0 h, the number of autophagosomes in *ein3/eil1-1,*

279 *cs16651* and *rbohd/f* mutants was significantly lower than in the WT. However, the number of

280 autophagosomes in *ein3/eil1-1* and *cs16651* mutants increased after 24 h of waterlogging and

281 had no significant difference compared to the WT (Fig. 4A-a). To further explore the role of

282 ethylene-induced autophagy in plant responses to waterlogging stress, WT seedlings were

283 observed by transmission electron microscopy. In the control group, cell morphology was

284 normal, and the cell wall, cell membrane, and mitochondrial morphology were intact. However,

285 in the other treatment groups, with the increase in treatment time, most of the mitochondrial

286 cristae were degraded, and some mitochondrial cristae had completely disappeared to form

287 vacuolar structures, and the number of mitochondria gradually decreased (Fig. 4B). In the early

288 stage of waterlogging (duration of continuous waterlogging less than 12 h), the WL+ACC

289 treatment group produced more autophagosomes, and more damaged mitochondria were cleared

290 earlier (Fig. 4A-b). After 24 h, vacuolated mitochondria in the cytoplasm were transported into

291 vacuoles via the autophagy pathway (Fig. 4B). In addition, ethylene-related mutants *ACS2*,

292 *ACS6*, *ein3/eil1-1*, and *cs16651* were waterlogged and then observed by electron microscopy

293 (*Fig. S4A*), and the number of mitochondrial lesions in the mutants was higher when waterlogged

294 for 4 h (*Fig. S4a*).

295 Effects of waterlogging on root cell activity

296 To further explore the physiological changes of plants in response to waterlogging stress, WT

297 seedlings were subjected to different treatments for PI staining and FDA staining to observe

298 changes in root cell activity. PI staining showed that the root cells did not die significantly at 0-

299 24 h (*Fig. S5A*), while FDA staining showed that the WL+ACC treatment group had higher cell

300 viability than the WL treatment group in the early stage of waterlogging (*Fig. S5B*). However,

301 long-term waterlogging stress leads to cell death and production of aerenchyma (*Fig. S6*).

302 **Discussion**

303 WL and ACC enhance ethylene signaling and negatively regulate *Arabidopsis* root

304 growth

305 Climate disasters, such as waterlogging, drought and high temperature, often cause huge losses

306 to agriculture. To resist waterlogging, plants have evolved complex mechanisms to adapt to

307   flooded environments. Studies have shown that ethylene not only rapidly accumulates in plant

308   tissues but also rapidly activates ethylene-induced physiological responses under flooding stress

309   conditions (Hartman, Sasidharan & Voesenek, 2021). Deep water induces the expression of

310   genes SNORKEL1 and SNORKEL2, which encode ethylene response factors involved in

311   ethylene signaling in rice and indirectly increase the length of rice internodes to enhance gas

312   exchange with water to adapt to flooding stress (Hattori et al., 2009). The interrelationship

313   between ethylene and ROS produced by plants under submerged conditions has been reported

314   less frequently in *Arabidopsis*. Compared to the control group, the ACC and WL-treated group

315   showed a significant increase in the number of damaged mitochondria in root cells (Fig. 4b),

316   which may have contributed to the relatively stunted growth observed in the treated seedlings

317   due to the crucial role of mitochondria in plant growth, suggesting negative regulation of root

318   growth by WL and ACC (Fig. 1B). It is speculated that the difference in root length between the

319   different treatment groups may be related to the ethylene content. To further explore the changes

320   in ethylene content after WL treatment, this study showed that the ethylene content of the WL

321   treatment group and ACC treatment group increased continuously with the treatment time.

322   Compared with the WL and ACC treatment groups, the ethylene content of the WL+ACC

323   treatment group did not increase significantly, but ethylene accumulated rapidly in the early

324   stage of treatment, reaching the maximum ethylene content at 8 h, and decreased after 12 h (Fig.

325   1C). Treatment with ACC in wheat seedlings can increase ethylene accumulation in the roots of

326   wheat seedlings and enhance the seedlings' tolerance to hypoxic conditions (Yamauchi et al.,

327   2014). It has also been reported that ethylene promotes root hair growth in *Arabidopsis* by

328   coordinating the activities of EIN3/EIL1 and RHD6/RSL1 (Feng et al., 2017). Salt and drought

329   stress can induce the expression of *MnEIL3*, which is a homologous gene of *ein3* in the roots and

330   shoots of mulberry, and *Arabidopsis* overexpressing *MnEIL3* showed enhanced tolerance to salt

331   and drought stress. Therefore, MnEIL3 may play an important role in abiotic stress resistance

332   (Liu et al., 2019). Using different treatments in *Arabidopsis* EIN3-GFP plants, the expression of

333   the EIN3 protein in *Arabidopsis* was significantly up-regulated in the WL and ACC treatment

334   groups, but the EIN3 protein in the WL+ACC treatment group was not significantly up-regulated

335   at 24 h (*Fig. S1*). The qRT-PCR data of ethylene-related genes further demonstrated that WL

336   treatment and ACC treatment enhanced ethylene signaling (Fig. 1D). The above experimental

337   results indicate that ethylene may only accumulate and play a role in the early stage of

338   waterlogging stress, and that plants may undergo adaptive morphological changes in the later

339   stage of waterlogging to respond to stress. However, further studies are needed to determine

340   which genes in the ethylene signaling pathway are involved in the regulation mechanism of plant

341   waterlogging stress.

342   ## The relationship between ethylene, ROS and autophagy under waterlogging stress

343   Ethylene plays an important role in inducing autophagy and reducing ROS in organisms, thereby

344   improving plant survival during flooding, hypoxia and reoxygenation stress (Hartman,

345   Sasidharan & Voesenek, 2021). This study showed that ACC could rapidly induce ROS

346   production in *Arabidopsis* under waterlogging stress (Fig. 2A). Additionally, studies have shown

347   that the expressions of GmATG8i, GmATG4, GmACC synthase, GmERF, and GmEin3 are up-

348   regulated in soybean seedlings under starvation stress, and starvation-induced autophagy may be

349   partially mediated by ethylene signaling (Okuda et al., 2011). In this study, the expression of

350   autophagy genes in *Arabidopsis* was up-regulated under waterlogging stress, and the

351   phenomenon of autophagy first appeared in the vascular column. Over time, the phenomenon of

352   autophagy was also found in the cortex of the root. Autophagy occurred only in the vascular

353   column in the roots under ACC treatment. Compared with the WL and ACC-treated groups, the

354   location and extent of autophagy in the WL+ACC treatment group were changed (Fig. 3B).

355   Various abiotic stressors, such as high salt, high temperature, drought, low temperature, and

356   hypoxia can induce autophagy, which plays an important role in balancing plant growth and

357   enhancing stress tolerance (Qi, Xia & Xiao, 2021). Additionally, this study found that the

358   number of autophagosomes in *ein3/eil1-1*, *cs16651*, and *rbohd/f* mutants were significantly

359   lower than that of the WT at 0 h (Fig. 4a). Therefore, we presumed that this explains the

360   difference in the number of autophagosomes and ROS content between the mutants (*Fig. S2A*).

361   ## Ethylene participates in the induction of ROS generation under waterlogging stress

362   Adventitious root formation is a response to plant adaptation to flooding stress, and ROS

363   signaling is involved in ethylene- and auxin-induced adventitious root formation in flooded

364   cucumber plants (Qi et al., 2020). However, the regulatory relationship between ethylene and

365   ROS under waterlogging stress remains unclear. Previous studies in the laboratory have

366   demonstrated that roots can produce ROS after waterlogging, and ROS is an important signal in

367   response to plant programmed cell death (Guan et al., 2019). WL and ACC treatments induced

368   ROS production in *Arabidopsis* (Fig. 2A). The ethylene content no longer increased after 12 h

369   (Fig. 1C), and the ROS content began to decrease in the ACC treatment group. The ROS content

370   is closely related to the ethylene content, and ACC treatment increased the $O_2^{\cdot-}$ content in the

371   roots (Fig. 2A-c). *Arabidopsis* treated with AVG (2-aminoethoxyvinyl glycine (an inhibitor of

372   ethylene synthesis)) had a reduced $O_2^{\cdot-}$ content in the roots (Lv et al., 2018). After the WL+ACC

373   treatment, the ethylene content and ethylene-related gene expression of WT plants decreased

374   with the increase in treatment time (Fig. 1C and 1D), but the ROS content generally increased

375   (Fig. 2A). The ethylene content of *cs16651* mutant plants did not change significantly under

376   waterlogging (*Fig. S2B*) but still produced ROS (*Fig. S2A*). Therefore, under waterlogging

377   conditions, ROS production has a certain dependence on ethylene, but the increase in ROS is not

378   completely dependent on ethylene. The decrease in ethylene content may also be due to

379   excessive ROS levels, which negatively regulates ethylene production. However, the relevant

380   regulatory mechanisms need further study.

381   Excessive accumulation of ROS activates the antioxidant system

382   Under normal circumstances, ROS in plants is maintained at a low level. When plants are

383   subjected to external environmental stress, ROS content increases, affecting the normal

384   metabolic microenvironment in plants (Wang et al., 2018b). Plants have evolved a relatively

385   complete scavenging system to maintain ROS balance (Gill & Tuteja, 2010). The activities of

386   SOD, CAT, APX, and GR of the submerged-tolerant varieties were higher than those of the non-

387   submerged varieties after 8 days of flooding treatment on rice. Rice can enhance the tolerance of

388   rice to flooding stress by improving its antioxidant system (Iskandar & Mahmood, 2010). In the

389   present study, compared with the WL treatment group, the WL+ACC-treated group had

390   relatively higher CAT1 and SOD1 enzymatic activities at the early stage of waterlogging (*Fig.*

391   *S3*), and *CAT1* and *SOD1* expression also occurred earlier (Fig. 2B), suggesting that excessive

392   ROS accumulation activates the antioxidant system. During the 24-48 h period, the plants were

393   in a waterlogged state, and the antioxidant system was insufficient to remove excess ROS. The

394   WL and WL+ACC treatment groups continued to accumulate ROS. However, further studies are

395   needed to determine which genes are involved in the regulation of the antioxidant system and

396   lead to the weakening of the activity of antioxidant enzymes.

397   **Conclusions**

398   In summary, ethylene can promote ROS production in the early stages of waterlogging (duration

399   of continuous waterlogging for less than 12 h), and plants remove excess ROS through the

400   antioxidant system, resulting in a temporary decrease in ROS content. With prolonged

401   waterlogging treatment time, the ROS content continued to rise (Fig. 2). When the antioxidant

402   systems of CAT1 and SOD1 enzymes were insufficient to remove excess ROS in plants (*Fig.*

403   *S3*), ethylene induced partial autophagy production, accelerating mitochondrial degradation to

404   reduce ROS production and alleviate oxidative damage in plants (Fig. 4B). The autophagy

405   pathway accelerates the degradation of mitochondria, which is essential for plants to alleviate

406   oxidative damage and increase survival in the early stage of waterlogging stress. However, long-

407   term waterlogging exacerbates mitochondrial degradation, resulting in cell death and the

408   production of aerenchyma (*Fig. S6*). The lack of adequate energy supply in plants leads to

409   restricted growth and development, and the shortened root length is a response to waterlogging

410   stress (Fig. 1B). The mechanism by which ethylene induces autophagy and accelerates

411   mitochondrial degradation is not fully understood. It is unclear to what extent ROS

412   accumulation induces autophagy to degrade mitochondria. Additionally, why does ethylene-

413   induced autophagy first occur in the vascular column and then spread to the root cortex after

414   waterlogging? These issues warrant further study and exploration.

415   Acknowledgements

416   We thank Prof. Zhaojun Ding (Shandong University) for octet *acs* mutant (*CS16651*, *acs2-*

417   *1/acs4-1/acs5-2/acs6-1/acs7-1/acs9-1/amiRacs8acs11*), *ein2-5*, *p35S::EIN3-GFP*, and *ein3/eil1-*

418   *1* seeds. We would like to thank LetPub (www.letpub.com) for providing linguistic assistance

419   during the preparation of this manuscript.

420   References

421   Chen L, Liao B, Qi H, Xie LJ, Huang L, Tan WJ, Zhai N, Yuan LB, Zhou Y, Yu LJ, Chen QF,
422   Shu W, Xiao S. 2015a. Autophagy contributes to regulation of the hypoxia response during
423   submergence in Arabidopsis thaliana. *Autophagy* 11:2233–2246. DOI:
424   10.1080/15548627.2015.1112483.
425   Chen L, Liao B, Qi H, Xie LJ, Huang L, Tan WJ, Zhai N, Yuan LB, Zhou Y, Yu LJ, Chen QF,
426   Shu W, Xiao S. 2015b. Autophagy contributes to regulation of the hypoxia response during
427   submergence in Arabidopsis thaliana. *Autophagy* 11:2233–2246. DOI:
428   10.1080/15548627.2015.1112483.
429   Feng Y, Xu P, Li B, Li P, Wen X, An F, Gong Y, Xin Y, Zhu Z, Wang Y, Guo H. 2017.
430   Ethylene promotes root hair growth through coordinated EIN3/EIL1 and RHD6/RSL1
431   activity in Arabidopsis. *Proceedings of the National Academy of Sciences of the United*
432   *States of America* 114:13834–13839. DOI: 10.1073/pnas.1711723115.
433   Foyer CH, Noctor G. 2003. Redox sensing and signalling associated with reactive oxygen in
434   chloroplasts, peroxisomes and mitochondria. *Physiologia Plantarum*:355–364. DOI:
435   10.1034/j.1399-3054.2003.00223.x.
436   Gill SS, Tuteja N. 2010. Reactive oxygen species and antioxidant machinery in abiotic stress
437   tolerance in crop plants. *Plant Physiology and Biochemistry* 48:909–930. DOI:
438   10.1016/j.plaphy.2010.08.016.
439   Guan B, Lin Z, Liu D, Li C, Zhou Z, Mei F, Li J, Deng X. 2019. Effect of waterlogging-induced
440   autophagy on programmed cell death in Arabidopsis roots. *Frontiers in Plant Science* 10:1–
441   16. DOI: 10.3389/fpls.2019.00468.

442 Hartman S, Liu Z, Veen H Van, Vicente J, Reinen E, Martopawiro S, Zhang H, Dongen N Van,
443   Bosman F, Bassel GW, Visser EJW, Bailey-serres J, Theodoulou FL, Hebelstrup KH, Gibbs
444   DJ, Holdsworth MJ, Sasidharan R, Voesenek LACJ. 2019. Ethylene-mediated nitric oxide
445   depletion pre-adapts plants to hypoxia stress. *Nature Communications* 10:4020. DOI:
446   10.1038/s41467-019-12045-4.
447 Hartman S, Sasidharan R, Voesenek LACJ. 2021. The role of ethylene in metabolic acclimations
448   to low oxygen. *New Phytologist* 229:64–70. DOI: 10.1111/nph.16378.
449 Hattori Y, Nagai K, Furukawa S, Song XJ, Kawano R, Sakakibara H, Wu J, Matsumoto T,
450   Yoshimura A, Kitano H, Matsuoka M, Mori H, Ashikari M. 2009. The ethylene response
451   factors SNORKEL1 and SNORKEL2 allow rice to adapt to deep water. *Nature* 460:1026–
452   1030. DOI: 10.1038/nature08258.
453 Iskandar R, Mahmood D. 2010. Responses of the antioxidative enzymes in Malaysian rice (
454   Oryza sativa L .) cultivars under submergence condition. *Acta Physiol Plant*:739–747. DOI:
455   10.1007/s11738-009-0456-3.
456 Kumar D, Yusuf M, Singh P, Sardar M, Sarin N. 2014. Histochemical Detection of Superoxide
457   and H2O2 Accumulation in Brassica juncea Seedlings. *BIO-PROTOCOL* 4:1108. DOI:
458   10.21769/bioprotoc.1108.
459 Li F, Vierstra RD. 2012. Autophagy: A multifaceted intracellular system for bulk and selective
460   recycling. *Trends in Plant Science*:526–537. DOI: 10.1016/j.tplants.2012.05.006.
461 Liu Y, He C. 2016. Regulation of plant reactive oxygen species (ROS) in stress responses:
462   learning from AtRBOHD. *Plant Cell Reports* 35:995–1007. DOI: 10.1007/s00299-016-
463   1950-x.
464 Liu C, Li J, Zhu P, Yu J, Hou J, Wang C, Long D, Yu M, Zhao A. 2019. Mulberry EIL3 confers
465   salt and drought tolerances and modulates ethylene biosynthetic gene expression. *PeerJ*
466   7:6391. DOI: 10.7717/peerj.6391.
467 Lv B, Tian H, Zhang F, Liu J, Lu S, Bai M, Li C, Ding Z. 2018. Brassinosteroids regulate root
468   growth by controlling reactive oxygen species homeostasis and dual effect on ethylene
469   synthesis in Arabidopsis. *PLoS Genetics* 14:1–26. DOI: 10.1371/journal.pgen.1007144.
470 Ma J, Liang Z, Zhao J, Wang P, Ma W, Mai KK, Andrade JAF. 2021. Friendly mediates
471   membrane depolarization-induced mitophagy in Arabidopsis. *Current Biology* 31:1931-
472   1944.e4. DOI: 10.1016/j.cub.2021.02.034.
473 Marshall RS, Vierstra RD. 2018. Autophagy: The Master of Bulk and Selective Recycling.
474   *Annual Review of Plant Biology* 69:173–208. DOI: 10.1146/annurev-arplant-042817-
475   040606.
476 Morel Y, Barouki R. 1999. Repression of gene expression by oxidative stress. *Biochemical
477   Journal* 342:481–496. DOI: 10.1042/0264-6021:3420481.
478 Mu P, Plaszczyca M, Plaszczyca M, Mellerowicz E, Karpinski S. 2007. Lysigenous Aerenchyma
479   Formation in Arabidopsis Is Controlled by LESION SIMULATING DISEASE1. *Acta
480   Physiol Plant* 19:3819–3830. DOI: 10.1105/tpc.106.048843.
481 Nguyen TN, Lazarou M. 2021. Plant mitophagy : Beware of Friendly or you might get eaten.
482   *Current Biology* 31:R457–R458. DOI: 10.1016/j.cub.2021.02.059.
483 Okuda M, Nang MPSH, Oshima K, Ishibashi Y, Zheng SH, Yuasa T, Iwaya-Inoue M. 2011. The
484   ethylene signal mediates induction of GmATG8i in soybean plants under starvationstress.
485   *Bioscience, Biotechnology and Biochemistry* 75:1408–1412. DOI: 10.1271/bbb.110086.
486 Parlanti S, Kudahettige NP, Lombardi L, Alpi A, Perata P, Pucciariello C. 2011. Distinct
487   mechanisms for aerenchyma formation in leaf sheaths of rice genotypes displaying a

488   quiescence or escape strategy for flooding tolerance. *Annals of Botany* 107:1335–1343.
489   DOI: 10.1093/aob/mcr086.
490 Perata P. 2020. Ethylene Signaling Controls Fast Oxygen Sensing in Plants. *Trends in Plant*
491   *Science* 25:3–6. DOI: 10.1016/j.tplants.2019.10.010.
492 Phukan UJ, Mishra S, Shukla RK. 2016. Waterlogging and submergence stress: affects and
493   acclimation. *Critical Reviews in Biotechnology* 36:956–966. DOI:
494   10.3109/07388551.2015.1064856.
495 Qi X, Li Q, Shen J, Qian C, Xu X, Xu Q, Chen X. 2020. Sugar enhances waterlogging-induced
496   adventitious root formation in cucumber by promoting auxin transport and signalling. *Plant,*
497   *Cell and Environment* 43:1545–1557. DOI: 10.1111/pce.13738.
498 Qi H, Xia FN, Xiao S. 2021. Autophagy in plants: Physiological roles and post-translational
499   regulation. *Journal of Integrative Plant Biology* 63:161–179. DOI: 10.1111/jipb.12941.
500 Sun X, Li Y, He W, Ji C, Xia P, Wang Y, Du S, Li H, Raikhel N, Xiao J, Guo H. 2017.
501   Pyrazinamide and derivatives block ethylene biosynthesis by inhibiting ACC oxidase.
502   *Nature Communications* 8:15758. DOI: 10.1038/ncomms15758.
503 Suzuki N, Miller G, Morales J, Shulaev V, Torres MA, Mittler R. 2011. Respiratory burst
504   oxidases: The engines of ROS signaling. *Current Opinion in Plant Biology*:691–699. DOI:
505   10.1016/j.pbi.2011.07.014.
506 Voesenek LACJ, Sasidharan R. 2013. Ethylene - and oxygen signalling - drive plant survival
507   during flooding. *Plant Biology* 15:426–435. DOI: 10.1111/plb.12014.
508 Wang W, Chen D, Zhang X, Liu D, Cheng Y, Shen F. 2018a. Role of plant respiratory burst
509   oxidase homologs in stress responses. *Free Radical Research* 52:826–839. DOI:
510   10.1080/10715762.2018.1473572.
511 Wang W, Chen D, Zhang X, Liu D, Cheng Y, Shen F. 2018b. Role of plant respiratory burst
512   oxidase homologs in stress responses. *Free Radical Research* 52:826–839. DOI:
513   10.1080/10715762.2018.1473572.
514 Wang X, Ma Q, Wang R, Wang P, Liu Y, Mao T. 2020. Submergence stress-induced hypocotyl
515   elongation through ethylene signaling-mediated regulation of cortical microtubules in
516   Arabidopsis. *Journal of Experimental Botany* 71:1067–1077. DOI: 10.1093/jxb/erz453.
517 Wang P, Mugume Y, Bassham DC. 2018. New advances in autophagy in plants: Regulation,
518   selectivity and function. *Seminars in Cell and Developmental Biology*:113–122. DOI:
519   10.1016/j.semcdb.2017.07.018.
520 Waszczak C, Carmody M, Kangasjärvi J. 2018. Reactive Oxygen Species in Plant Signaling.
521   *Annual Review of Plant Biology*:209–236. DOI: 10.1146/annurev-arplant-042817-040322.
522 Xie L, Chen Q, Chen M, Yu L, Huang L, Chen L, Wang F, Xia F, Zhu T, Wu J, Yin J, Liao B,
523   Shi J, Zhang J, Aharoni A, Yao N, Shu W, Xiao S. 2015. Unsaturation of Very-Long-Chain
524   Ceramides Protects Plant from Hypoxia-Induced Damages by Modulating Ethylene
525   Signaling in Arabidopsis. *PLoS Genetics* 11:1–33. DOI: 10.1371/journal.pgen.1005143.
526 Yamauchi T, Watanabe K, Fukazawa A, Mori H, Abe F, Kawaguchi K, Oyanagi A, Nakazono
527   M. 2014. Ethylene and reactive oxygen species are involved in root aerenchyma formation
528   and adaptation of wheat seedlings to oxygen-deficient conditions. *Journal of Experimental*
529   *Botany* 65:261–273. DOI: 10.1093/jxb/ert371.
530 Yamauchi T, Yoshioka M, Fukazawa A, Mori H, Nishizawa NK, Tsutsumi N. 2017. An NADPH
531   Oxidase RBOH Functions in Rice Roots during Lysigenous Aerenchyma Formation under
532   Oxygen-De fi cient Conditions. *The Plant cell* 29:775–790. DOI: 10.1105/tpc.16.00976.

533 Yao Y, He RJ, Xie QL, Zhao X, Deng X, He J, Song L, He J, Marchant A, Chen X, Wu A, Chen
534   X. 2017. ETHYLENE RESPONSE FACTOR 74 (ERF74) plays an essential role in
535   controlling a respiratory burst oxidase homolog D (RbohD) -dependent mechanism in
536   response to different stresses in Arabidopsis. *New Phytologist* 213:1667–1681. DOI:
537   10.1111/nph.14278.
538 Yeung E, Bailey-serres J, Sasidharan R. 2019. After The Deluge : Plant Revival. *Trends in Plant*
539   *Science* 24:443–454. DOI: 10.1016/j.tplants.2019.02.007.
540 Yu F, Liang K, Fang T, Zhao H, Han X, Cai M, Qiu F. 2019. A group VII ethylene response
541   factor gene , ZmEREB180 , coordinates waterlogging tolerance in maize seedlings. *Plant*
542   *Biotechnology Journal* 17:2286–2298. DOI: 10.1111/pbi.13140.
543 Zhang H, Bosch-Marce M, Shimoda LA, Yee ST, Jin HB, Wesley JB, Gonzalez FJ, Semenza
544   GL. 2008. Mitochondrial autophagy is an HIF-1-dependent adaptive metabolic response to
545   hypoxia. *Journal of Biological Chemistry* 283:10892–10903. DOI:
546   10.1074/jbc.M800102200.
547 Zhu JK. 2016. Abiotic Stress Signaling and Responses in Plants. *Cell* 167:313–324. DOI:
548   10.1016/j.cell.2016.08.029.
549 Zhu T, Zou L, Li Y, Yao X, Xu F, Deng X, Zhang D, Lin H. 2018. Mitochondrial alternative
550   oxidase-dependent autophagy involved in ethylene-mediated drought tolerance in Solanum
551   lycopersicum. *Plant Biotechnology Journal* 16:2063–2076. DOI: 10.1111/pbi.12939.
552

Figure 1

Dynamics of ROS, H_2O_2 and O^- changes in *Arabidopsis* roots under different treatments (A-B).

(a)ROS fluorescence probe H_2DCFH-DA was used to detect the changes of ROS in the roots of 7-day-old WT seedlings under different treatment, scale bar =25 μm.(b)DAB staining was used to detect the changes of H_2O_2 in the roots of 7-day-old WT seedlings under different

treatment, scale bar =50 μm.(c)NBT staining was used to detect the changes of O^- in the roots of 7-day-old WT seedlings under different treatment, scale bar =50 μm.(d-e-f)Relative staining intensities calculated from *Fig. 2A-a-b-c* . (B)QRT-PCR detected the relative expression of antioxidase related genes (*SOD1*, *CAT1* and *GST1*) in 7-day-old WT seedlings under different treatments. All of the experiments were performed for three biological replications. Data shown are the mean ± SD (n = 3). ＊ P < 0.05; ＊＊ P < 0.01; ＊＊＊ P < 0.001 by Student's t-test.
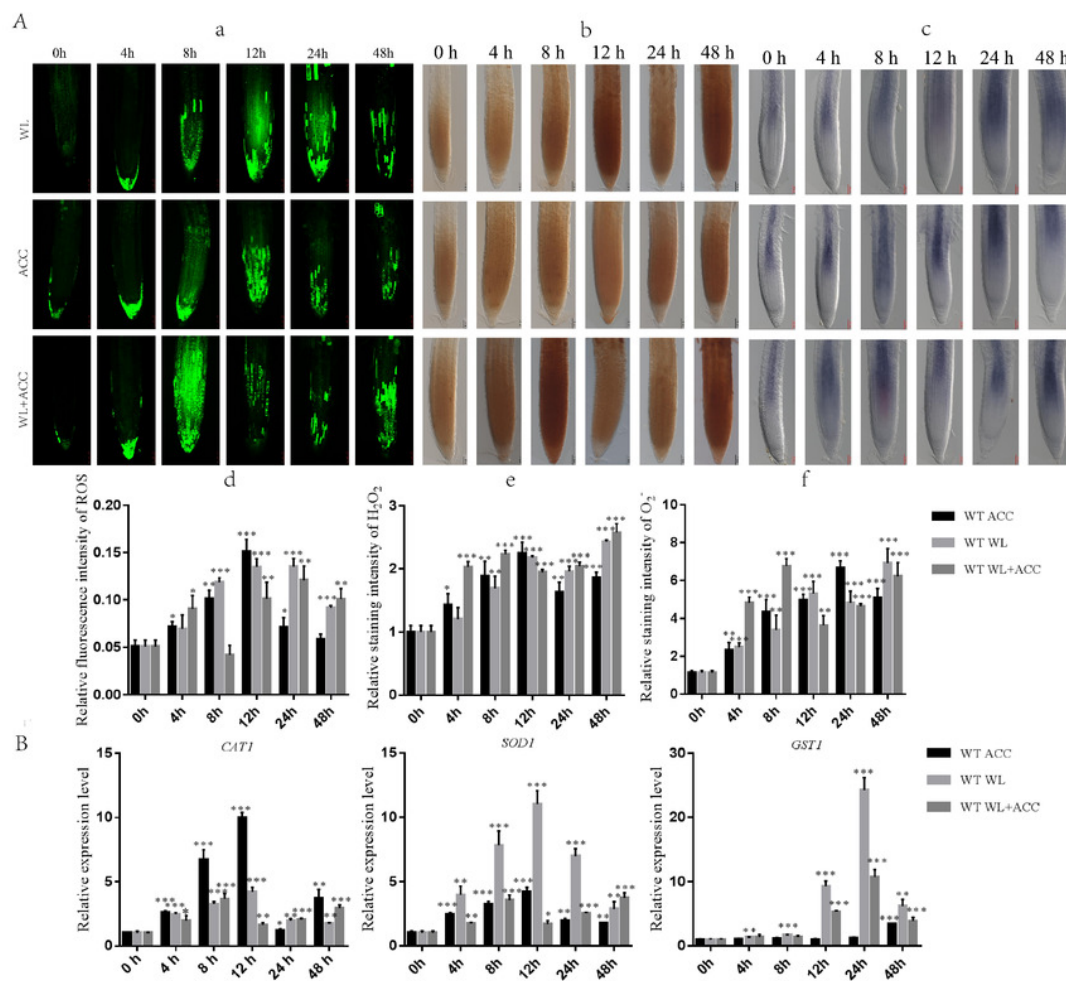
Figure 2

Phenotypic analysis of 7-day WT seedlings under different treatments(A-D).

(A) The phenotype of 7-day-old WT seedlings under different concentrations of ACC solution, scale bar = 1 cm. (a) Statistical analysis of the root length in *Fig. 1A*. (B) Phenotypic changes in root length of 7-day-old WT seedlings under different treatments for 48 h, scale bar = 1 cm. (b) Statistical analysis of the root length in *Fig. 1B*.(C) Quantification of the relative ethylene production (compared to 0 h) of 7-day-old WT seedlings under different treatments at different time points. (D) QRT-PCR analyses showing the relative expression of ethylene-related genes (*ACO2, ACS2, ERF72, ERF73* and *EIN3*) in 7-day-old WT seedlings under different treatments at different time points. All of the experiments were performed for three biological replications. Data shown are the mean ± SD (n = 3). $*$ P < 0.05; $**$ P < 0.01; $***$ P < 0.001 by Student's t-test.
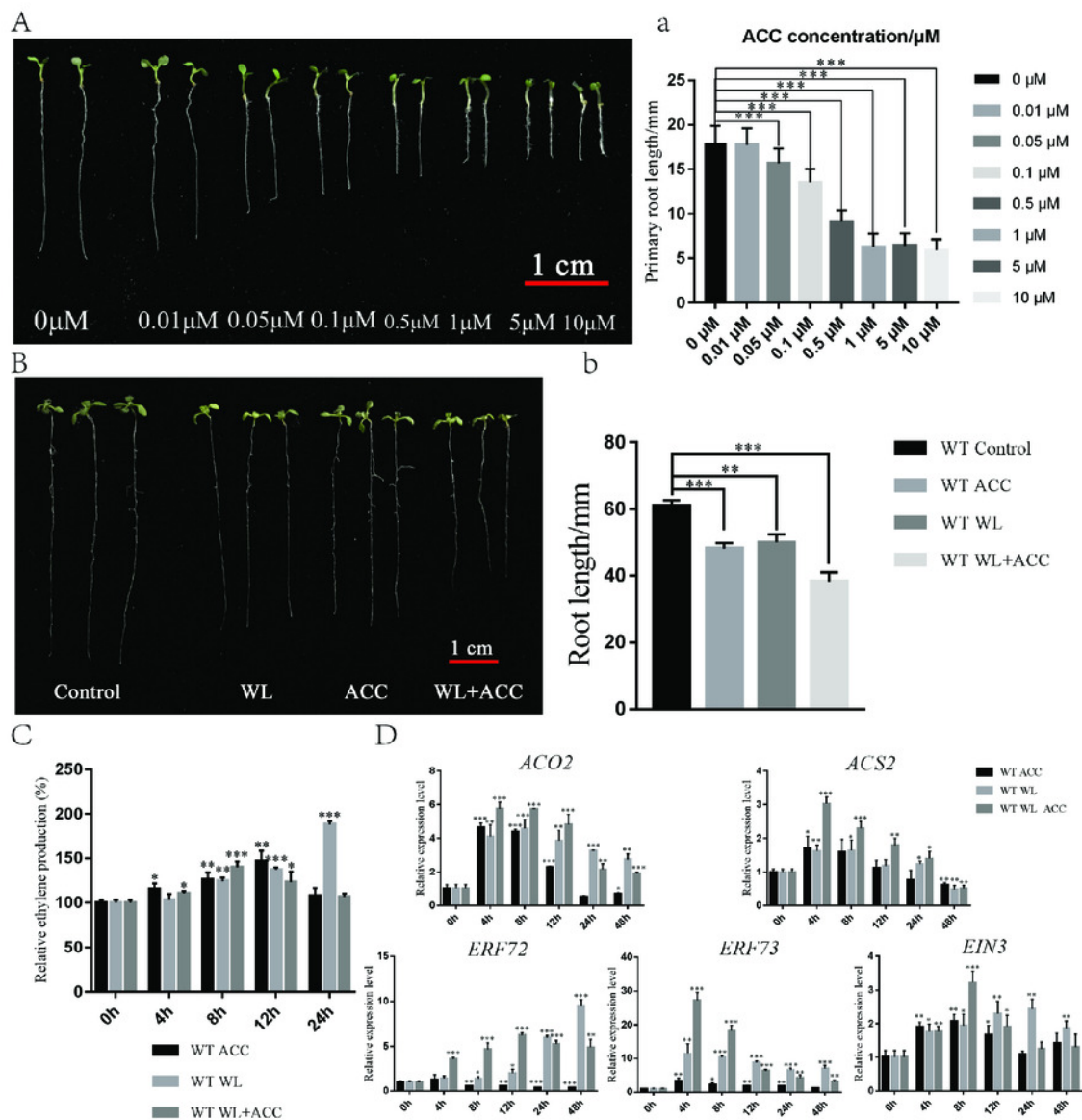
Figure 3

Ethylene induces autophagy in *Arabidopsis* roots under flooding stress (A-C).

 A QRT-PCR detected the relative expression of autophagy-related genes *ATG2, ATG5, ATG7, ATG8e*, and *ATG10* in 7-day-old WT seedlings under different treatments. B The expression of the *ATG8epro::GUS* reporter was monitored in WT roots under different treatments, scale bar = 50 μm. C Autophagosomes in roots of 7-day-old WT seedlings were observed by confocal microscopy after MDC staining under different treatments, scale bar = 75 μm. D The data is according to the statistics of the number of autophagosomes in *Fig. 3C*. All of the experiments were performed for three biological replications. Data shown are the mean ± SD (n = 3). ＊ P < 0.05; ＊＊ P < 0.01; ＊＊＊ P < 0.001 by Student's t-test.
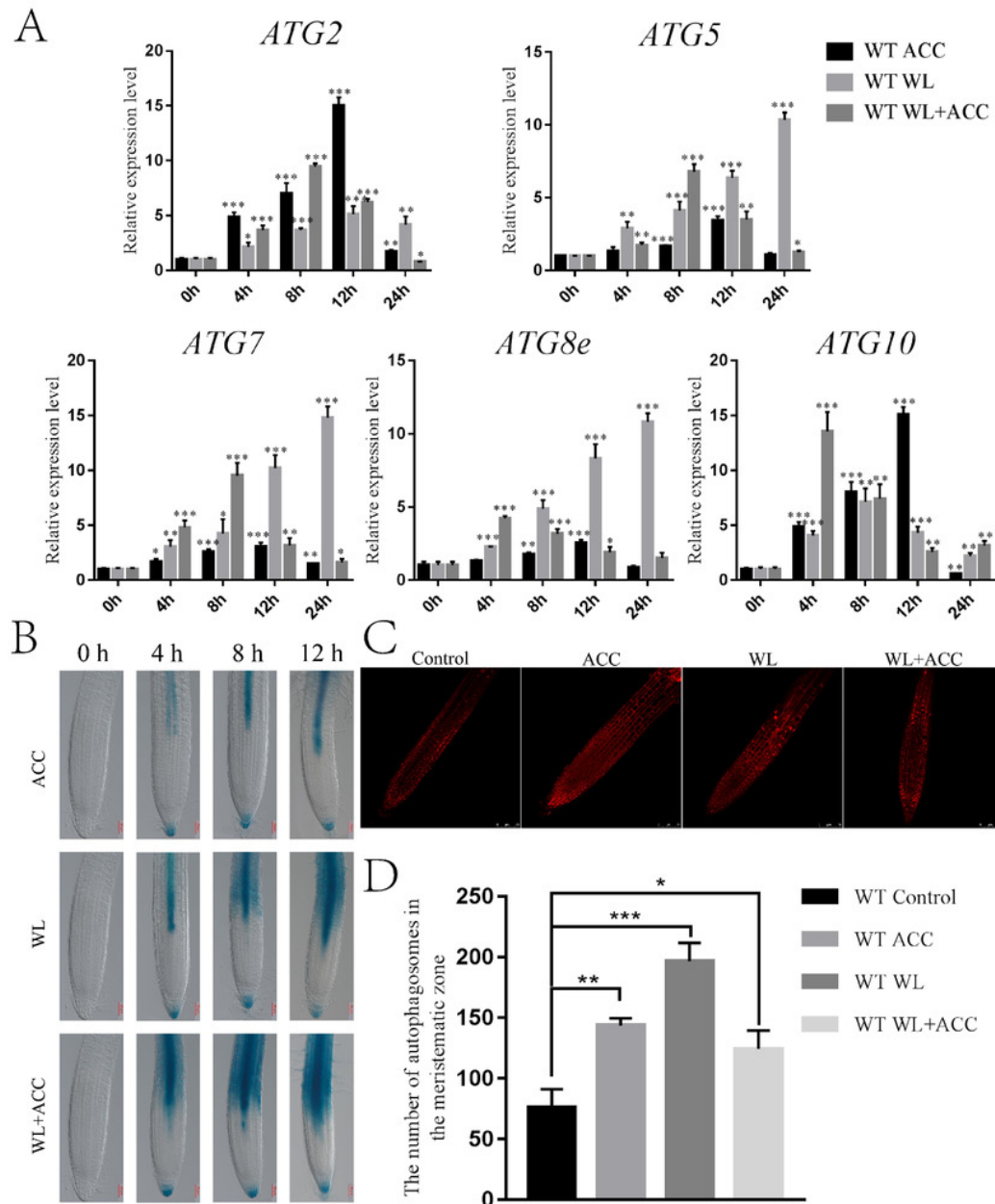
Figure 4

Observation on the ultrastructure of *Arabidopsis* root cells in different treatments (A-B).

(A)WT seedlings, *ein3/eil1-1*, *CS16651*, and *rbohd/f* mutants seedlings were stained with MDC under waterlogging treatment and then were used to observe autophagosomes, scale bar=75 μm.(a)The data is according to the statistics of the number of autophagosomes in *Fig. 4A*.(B)That ultrastructure of the roots of WT seedlings under different treatments was observed with a transmission electron microscopy. Arrows indicate autophagosomes or autophagic structures. CW, cell wall; M, mitochondrion or degraded mitochondria; ER, Endoplasmic reticulum; G, Golgi; V, Vacuole. Scale bar = 1μm.(b)The data is according to the statistics of the number of autophagosomes and the ratio of damaged mitochondria to intact mitochondria in a single cell in *Fig. 4B*. All of the experiments were performed for three biological replications. Data shown are the mean ± SD (n = 3). ∗ P < 0.05; ∗∗ P < 0.01; ∗∗∗ P < 0.001 by Student's t-test.